Self-heat effect of the thermistors in the VSL water calorimeter

A study of self-heat measurement by using different measuring and analyse techniques.

By David Mostert

D. Mostert
Delft August 2014

Supervisors:
L.A. de Prez MSc

C.A. Swarts
R.A. Mantel

Dutch Metrology Institute

VSL
Thijsseweg 11
2629 JA Delft
Postbus 654
2600 AR Delft
Netherlands

T +31 15 269 15 00
F +31 15 261 29 71
E info@vsl.nl
I www.vsl.nl

This work has been carried out by:
David Mostert
On request of: VSL
For the applicant: Leon de Prez

Summary

This report describes the work that has been done on the water calorimeter project at VSL. The calorimeter determines the absorbed-dose-to water D_w in gray, by measuring the radiation induced temperature change. The temperature of the water will change due to irradiation of a beam ionizing radiation. The irradiation causes a temperature difference. The temperature change of the water is determined with thermistors.

Each thermistor is connected to a digital multi-meter (DMM) to measure the resistance of the thermistor. The resistance is determined by measuring the voltage across the thermistor. The temperature change of the water can be determined with the resistance of the thermistor. The DMM supplies a measurement current through the thermistor. Power is dissipated because of the resistance of the thermistor. Therefore heat will be dissipated by the thermistor. This effect is called self-heat.

This report describes various measurements that where done to determine the so called self-heat of the thermistors in the water calorimeter. It is important for the dose measurements to be able to describe the behavior of the self-heat. The behavior of the self-heat can be described by convection, conduction, absorption and radiation. The self-heat is described by means of two types of least square fits. The fitting parameters are determined with an uncertainty to understand the self-heat behavior of the thermistors. The uncertainty in the self-heat is determined with use of a comprehensive uncertainty budget for each fitting equation.

The DMM can measure the resistance change of the thermistor with or without use of the OCOMP on setting or the OCOMP off setting. OCOMP represents offset compensated ohms. The OCOMP setting has influence on the self-heat of the thermistor; therefore it is also important to determine the behaviour of the OCOMP setting.

The self-heat is determined by measuring the temperature of the thermistor at different current values with a constant water temperature. This is done by two different measuring methods. The first measuring techniques use an external constant (DC) current source. The dissipated power in the thermistor is changed by changing the input current of the source. The second techniques use parallel resistors to change the dissipated power in the thermistors. The second measurement technique uses the input current of the DMM's; therefore it is possible to determine the self-heat with OCOMP on and OCOMP off.

The self-heat is determined for four different thermistors at OCOMP on and OCOMP off. The ratio between OCOMP on and OCOMP off is determined on the basis of the self-heat constants. The self-heat during a measurement with OCOMP on is less because of the offset compensation. The ratio between OCOMP on and OCOMP off is determined 16 times. The average ratio for the relevant thermistors between the self-heat at OCOMP on and OCOMP off is 0.86 ±0.10 (k=2). The self-heat constants have a value between 1.3 and 2.1 mK/µW. The uncertainty for the first fitting method is: 8.1 % and for the second fitting method: 6.5%.

Table of contents

List of figures

List of tables

1 Introduction

The unit gray (Gy) is the unit of interest when it comes to ionizing radiation. This unit can be realized by using water calorimetry. Since 2001 VSL has been operating a water calorimeter. The water calorimeter was used as the primary standard for the absorbed-dose-to-water in the Netherlands. The VSL water calorimeter is also the foundation for the NCS-18 dosimetry protocol. This protocol is applied by medical physicists in Belgium and the Netherlands [11].

Radiation beams are calibrated in terms of the absorbed-dose-to-water. Institutes use secondary standards for routine measurements to calibrate the radiation source. Ionization chambers are used as a secondary standard for absorbed dose. The primary standard in the Netherlands for absorbed-dose-to water is based on the water calorimeter (WCM).

Radiotherapy is continually advancing and new treatment methods are developed such as proton therapy and MRI linacs [7]. This led to the development of a new water calorimeter at VSL. This development was started in 2011 and the new water calorimeter was designed and constructed in 2013.

The first measurements at VSL with the new water calorimeter were done at the beginning of 2014. The results correspond with the results of the previous water calorimeter. Figure 1 and 2 show photos of the new water calorimeter during a measurement at the Netherlands Cancer Institute (NKI) in Amsterdam in august 2014. The WCM is placed horizontal in the beam of a linear particle accelerator.

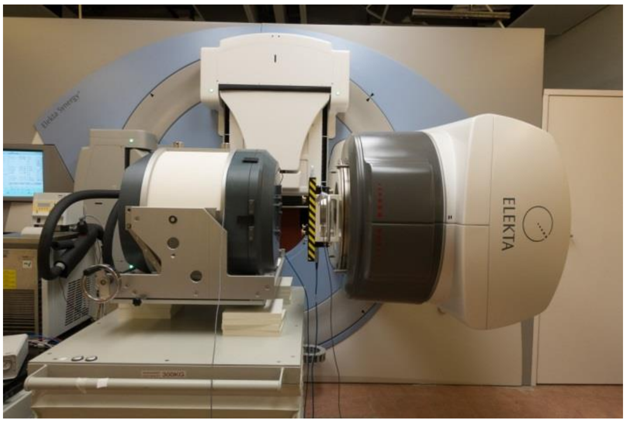

Figure 1: The WCM placed horizontal in the beam of a linear particle accelerator.

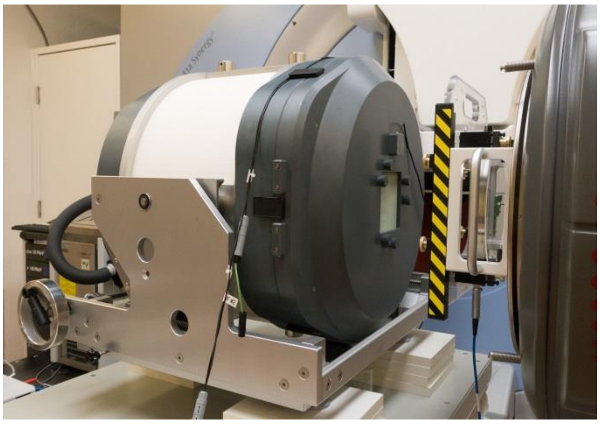

Figure 2: The WCM during a measurement set up at the NKI.

A water calorimeter consists of a tank with demineralized water, a so called water phantom. This phantom can be placed in a beam of ionizing radiation as shown in figure 1 and 2. Due to the irradiation the temperature of the water will rise.

The WCM realizes the absorbed-dose-to-water in the unit Gray (Gy). The ICRU (International Commission on Radiation measurements and Units) choses water as the standard reference material because the absorption and scattering properties are similar to that of human tissue [10].

The water calorimeter is based on temperature change due to irradiation. The temperature of the water will rise with approximately 0.24 mK per Gy. This temperature change needs to be determined with an absolute uncertainty less than 1 µK.

The water will absorb energy from the beam and the absorbed energy can be determined by measuring the temperature change of the water [1]:

$$D_w = c_{p,w} \cdot \Delta T_w \cdot \Pi k \tag{1}$$

With:

D_w	the absorbed-dose-to-water	[Gy]
$c_{p,w}$	the specific heat capacity of water at constant pressure	[4207, 5 J/kg·K]
ΔT_w	the temperature change due to radiation	[K]
Πk	product of correction factors	[-]

The temperature change of the water is determined with thermistors. One of the effects of a thermistor that influence the temperature change measurement is self-heat. This study is done to determine the effects of self-heat and to describe the behaviour of self-heat. The effect of self-heat on the temperature change measurements is described by the self-heat correction k_{sh} . k_{sh} is one element of the product of the correction factors Πk. The effect of the self-heat on the temperature change measurement is described by equation (2) [6].

$$\Delta T_w = \Delta T \cdot k_{sh} \tag{2}$$

Where ΔT is the temperature change of the thermistor. A previous study shows that a self-heat of 100 mK results in a self-heat correction factor of 1.0043. This results in a response change of 0.43 % in the thermistor. This study will describe the self-heat effect and is done to ensure new information about the self-heat behaviour and the parameters that will have influence on the self-heat.

2 The water calorimeter and the thermistors

The water calorimeter consists of different components. This chapter describes the important components related to this research and the behavior of the thermistor probes including the self-heat effect of the thermistors.

2.1 The water calorimeter

The absorbed-dose-to-water is measured with the water calorimeter. A cross section of the water calorimeter is shown in figure 3. The dose measurements are carried out at a water temperature of approximately 4 °C. The reason the measurement takes place at this temperature is because of the high density of the water at 4 °C. The density of water has a maximum at 4 °C. Therefore differences in temperature will not lead to convection. The convection in the water phantom is therefore assumed to be negligible [6].

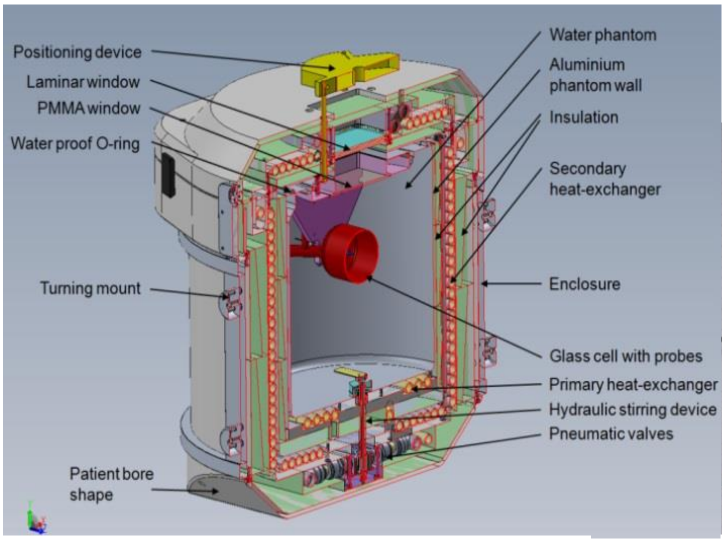

Figure 3: Cross section of the water calorimeter [6].

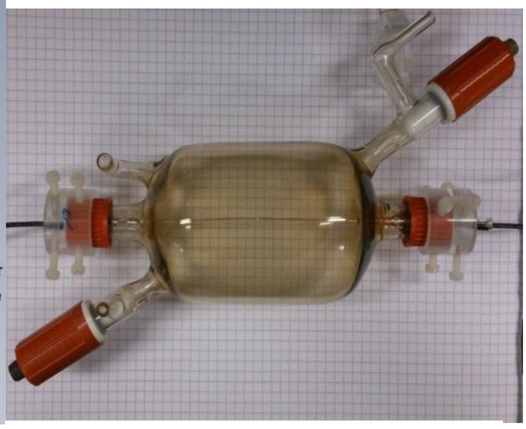

Figure 4: A picture of the HPC cell with the thermistor probes on the inside.

A primary heat exchange is mounted underneath the water phantom. The primary heat exchange system ensures that the temperature of the water is brought to 4 °C. The secondary heat-exchanger is used to maintain a stable temperature once the primary heat exchanger has brought the water temperature to 4 °C. Both heat-exchangers consist of a polyethylene tube. Cooling water is flowing through the polyethylene tubes to bring the water temperature to the desired temperature. The positions of the heat-exchangers are shown in figure 3. A stirring device is mounted at the bottom of the water phantom. The stirrer ensures that the heat transfer due to the primary system will be going faster and is distributed through the water phantom.

The measurement of the temperature change of the water takes place in the glass cell shown in figure 4. Two thermistor probes are mounted inside the cell. The glass cell (also known as the High Purity Cell or HPC) is filled with ultra-pure water. The ultra-pure water is taken from a Millipore MilliQ water purification system. A picture of the HPC is shown in figure 4. As shown in figure 4, the probes are attached in the middle of the HPC. One thermistor probe is positioned on the left opening and the other on the right opening.

The distance between the tips of the two probes is 1 cm. The probes are positioned at the reference depth, depending on the radiation beam quality [8]. The HPC is placed in the water phantom as shown in figure 3. The cell shown in figure 4 is the cell that is used at VSL for the absorbed-dose-to-water measurements.

2.2 Thermistor probes

The water temperature of the WCM will rise due to irradiation. Thermistors are used to measure the temperature change of the water due to irradiation. The word thermistor is a combination of the words "thermal resistor". The resistance of the thermistor will change as function of the temperature. Negative temperature coefficient (NTC) thermistors are used in the WCM. When the temperature rises the resistance will drop. The nominal resistance of the NTC is 10 kΩ at 4°C. Approximately the resistance will decrease with 4.3 %/K.

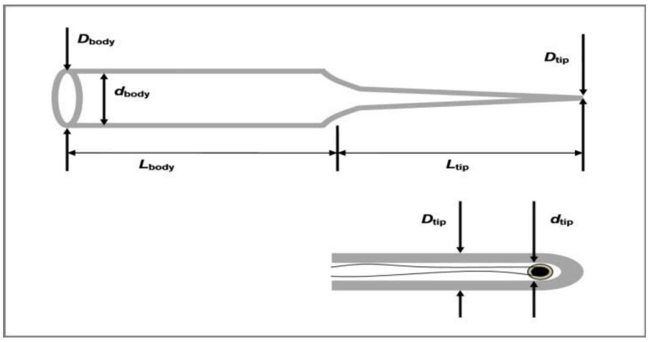

Figure 5: Technical drawings of the thermistor probe.

A technical drawing of a thermistor probe and a photo are shown in respectively figure 5 and figure 6. The thermistor probes are assembled at VSL and consist of a glass pipette with a closed tip. The thermistor itself is located in the tip of the glass pipette as shown in figure 5. The diameter of the thermistor is approximately 0.3 mm. The outer diameter of the pipette's body D_{body} is 6 mm and the inner diameter of the body d_{body} is 4 mm. The outer diameter of the tip of the pipette is 0.60 ± 0.15 mm. The total length of the body L_{body} is 55 ± 5 mm. The total length of the tip L_{tip} is 45 ± 5 mm [1].

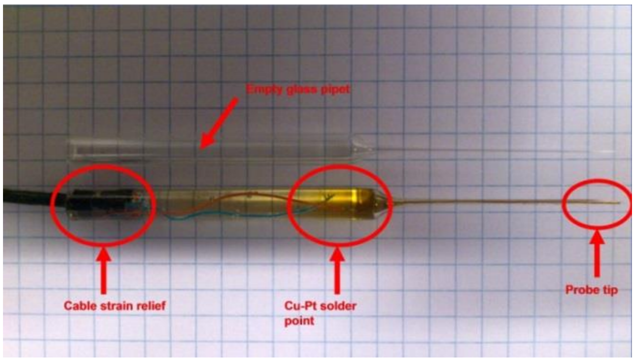

Figure 6: Photo of a thermistor probe.

Equation (3) describes the relation between the resistance of the thermistor and the absolute temperature of the thermistor [6].

$$R = R_\infty \cdot e^{\beta\left(\frac{1}{T}\right)} \tag{3}$$

With:

T	the temperature of the thermistor	[K]
β	the thermistor constant	[K]
R	the thermistor resistance as function of the temperature	[Ω]
R_∞	the thermistor resistance at infinite temperature	[Ω]

Equation (3) can be written as:

$$R = R_0 \cdot e^{\beta\left(\frac{1}{T}-\frac{1}{T_0}\right)} \tag{4}$$

This means that the temperature of the thermistor is equal to:

$$T = \left(\frac{1}{\beta}\ln\left(\frac{R}{R_0}\right) + \frac{1}{T_0}\right)^{-1} \tag{5}$$

R_0 represents the resistance of the thermistor at temperature T_0, 277.15 K. The thermistor constant β can be provided by the resistance versus temperature calibration. The thermistor constant β is expressed as the slope of the $1/T$ versus $\ln(R/R_\infty)$ curve. The value for β, T_0 and $R_0$are determined by a resistance versus temperature calibration.

Equation (5) shows the relation between the temperature and the resistance of the thermistor. With this expression it is possible to calculate the temperature after measuring the resistance of the thermistor.

2.3 The self-heat effect of the thermistor probes

Because of the increasing temperature change due to irradiation, it is important to determine effects that will have influence on the temperature of the thermistor and the water surrounding it. One of the effects that will occur is self-heat.

Each thermistor is connected to an Agilent digital multi-meter (DMM). When measuring the temperature of the water the DMM will supply a measurement current of 100 µA through the thermistor. Power is dissipated in the thermistor because of its resistance. This effect is called self-heat. The self-heat causes a difference between the actual water temperature and the temperature of the thermistor. The temperature change due to the self-heat depends on the probe construction and the dissipated power. The thermistor self-heat can be expressed as the difference between the thermistor temperature and the temperature of the medium:

$$\Delta T_{sh} = T - T_m \tag{6}$$

Where ΔT_{sh} is the temperature change of the thermistor due to self-heat, T is the thermistor temperature and T_m is the temperature of the medium. In this case the medium is the surrounding water.

The temperature of the water is brought to 4 °C as mentioned before. This is done to make the effect of convective heat transfer in the water phantom negligible. The self-heat, with absence of convective heat transfer in the water phantom, can be described by the self-heat constant c_{sh} in K/W and the dissipated power in the thermistor [1]. In this case the temperature change due to the self-heat of the thermistor can be described by the following equation:

$$\Delta T_{sh} = c_{sh} \cdot P \tag{7}$$

P is the dissipated electrical power in the thermistor. Practice shows that convection will occur despite the water temperature of 4 °C. The reason of the convection is the self-heat of the thermistor [3].

As a result of the current, an electrical power P is dissipated in the thermistor. An amount of electrical power is absorbed by the thermistor P_{ab}. The rest of the power is transferredto the surrounding medium by thermal conduction P_{cd}, convection P_{cv} and radiative heat transport P_{tr}. Therefore the dissipated power of the thermistor can be described by the following expression [2]:

$$P = P_{ab} + P_{cd} + P_{cv} + P_r \tag{8}$$

Because of the small surface area of the thermistor probe and the small temperature difference of approximately 100 mK, the contribution of radiative heat transport is negligible [2]. The other two terms can be described by the heat transfer coefficients h_{cd} and h_{cv}. The conductive transfer coefficient h_{cd} is inversely proportional to the self-heat constant c_{sh}.

The dissipated electrical power in the thermistor as function of time is described by:

$$P(t) = [m \cdot C]_{th} \frac{dT}{dt} + h_{cd} \cdot \Delta T_{sh}(t) + h_{cv} \cdot \Delta T_{sh}(t) \tag{9}$$

ΔT_{sh}	the self-heat of the thermistor	[K]
h_{cd}	thermal conduction transfer coefficient equal to $1/c_{sh}$	[$W \cdot K^{-1}$]
h_{cv}	thermal convection transfer coefficient	[$W \cdot K^{-1}$]
P	the dissipated power of the thermistor	[W]
$[m \cdot C]_{th}$	the heat capacitance of the thermistor probe	[$J \cdot K^{-1}$]
$\frac{dT}{dt}$	the temperature change of the thermistor probe per time unit	[$K \cdot s^{-1}$]
c_{sh}	the self-heat constant	[K/W]

Equation (9) is time dependent. It describes the behaviour of the dissipated power in relation to the temperature change of the thermistor.

The self-heat of the thermistor is the driving force for convection in the water [3]. The self-heat of the thermistor causes a temperature difference between the temperature of the water and the temperature of the thermistor. A difference in temperature between the water and the thermistor causes a difference in density. The difference in density creates a flow, so called convection and therefore a heat transfer. The movement of the water causes a heat flow. This heat flow causes the thermistor probe to cool down. This effect is described by the convective heat transfer coefficient.

The self-heat causes thermal convection. If it is assumed that the convection is proportional to the temperature difference between the water and the thermistor, than the thermal convection is proportional to the self-heat of the thermistor. Therefore the thermal convection transfer coefficient can be written as:

$$h_{cv} = v \cdot \Delta T_{sh} \tag{10}$$

v is the convection parameter in $W \cdot K^{-2}$.

The absorbed heat by the thermistor is described by the term: $[m \cdot C]_{th} \frac{dT}{dt}$. Combining equation (9), equation (10) and $t \rightarrow \infty$, gives the following equation for the dissipated power in the thermistor in a stationary condition :

$$P = h_{cd} \cdot \Delta T_{sh} + v \cdot \Delta {T_{sh}}^2 \tag{11}$$

The total dissipated power in the thermistor can be written as:

$$P = \frac{1}{c_{sh}} \cdot \Delta T_{sh} + v \cdot \Delta {T_{sh}}^2 \tag{12}$$

Equation (12) shows the simplified equation for the dissipated power in the thermistor. The equation is valid when the temperature of the thermistor is in a steady state. Chapter 3 describes another effect that must be taken into account, the so called background drift.

2.4 The digital multimeters and the OCOMP function

The thermistors are connected to two Agilent 3458A digital multimeters. Because of the small decrease of the resistance due to self-heat, the measurement needs to be done accurately. The Agilent digital multimeters are connected to the thermistor using a four wire resistance circuit. A schematic view of the circuit of one thermistor is shown in figure 7. The DMM generates a source current that will go through the thermistor and measures the voltage over the thermistor as shown in figure 7.

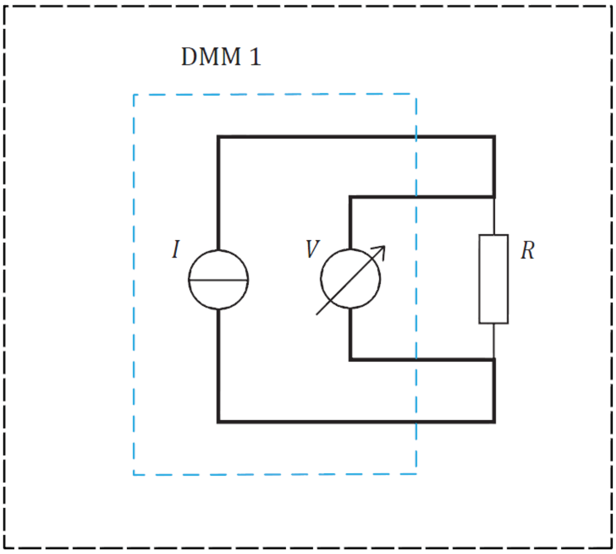

Figure 7: Schematic view of the measurement circuit of one thermistor with resistance *R*, the input current *I* and the voltage over the thermistor *V* [9].

An important function of the DMMs is the OCOMP function. OCOMP stands for offset compensated ohms. When using the OCOMP function, the DMM wil measure the voltage over the thermistor with and without a source current going through the thermistor. The induced voltage of the thermistor is equal to the difference between both measurements. When OCOMP is switched off, the DMM will only measure the voltage during a constant input source current [2]. The input current of OCOMP on is shown in figure 8 .

The OCOMP function influences the self-heat of the thermistor. As seen before, the current through the thermistor results in a dissipated power and therefore the themperature of the thermistor will increase. When OCOMP is on, the current is periodically switched off. Therefore the total self-heat will be less compared to a measurement with OCOMP off. Figure 8 illustrates the behaviour of the self-heat temperature of the thermistor [2]. Figure 8 is an approximation of the self-heat behaviour with OCOMP on and OCOMP off.

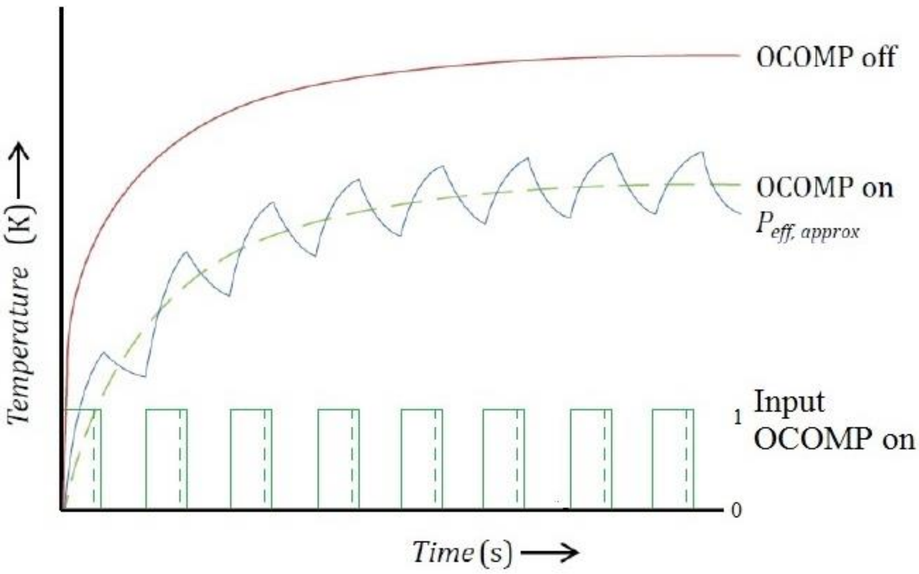

Figure 8: An approximation of the temperature change with OCOMP off (red line) and OCOMP on (blue line) [2].

During a measurement with OCOMP off the temperature of the thermistor will increase to a certain value due to the self-heat. With OCOMP on, the input current is block shaped as shown in figure 8. The thermistor only heats up when the input current is on and cools down when the input current is switched off. Therefore the thermistor temperature will increase less in relation to a measurement with OCOMP off. With OCOMP on the dissipated power in the thermistor is less. The dissipated power with OCOMP on can be described by the effective power dissipation P_{eff}. P_{eff} can be described as a percentage or ratio of the dissipated power with OCOMP off.

The dotted lines in the input graph of the OCOMP on, shows the moment when the DMM measures the resistance of the thermistor. The measurement sequence of the DMMs will have influence on P_{eff}. The up and down time of the DMM will affect the effective dissipated power of the thermistor and therefore the self-heat of the thermistor. If the DMM reads the resistance of the thermistor at the end of a sequence, P_{eff} will be higher. Thus the self-heat will be more. This behaviour is unknown, but through this research more information can be provided about this behaviour.

It is important to understand the behaviour of the self-heat with OCOMP on and OCOMP off. The self-heat influences the thermistor response, affecting the actual absorbed-dose measurement. The difference between the OCOMP on and OCOMP off self-heat can provide information about the OCOMP function and the behaviour of the thermistor.

The ratio between OCOMP on and OCOMP was unknown before this research. The ratio between OCOMP on and OCOMP off can be determined by the ratio between the self-heat at OCOMP on and the self-heat at OCOMP off.

3 Measurement methods and materials

The self-heat gives information about the behavior of the temperature of the thermistor. The self-heat behavior, described in § 2.3, determines the change of temperature due to the power dissipated in the thermistor. The temperature of the thermistor is measured at different current values and therefore at different power values.

As mentioned before it is important to understand and measure the behavior of the OCOMP function. The self-heat constant at OCOMP on and OCOMP off can give a lot of information about the OCOMP function. Therefore it is important to find an accurate way for measuring the self-heat.

3.1 Self-heat measurement with the Keithley power source.

The first self-heat measurement is done with an external Keithley current source. Figure 9 shows the measurement circuit. The two thermistors are connected to the current source. Due to the current a power is dissipated in the thermistor and the temperature of the thermistor will increase. The purpose of this study is to measure the self-heat of the two thermistors. Each thermistor is connected to a digital multimeter. The two DMM's that are used for this measurement are labelled with DMM 23 and DMM 24.

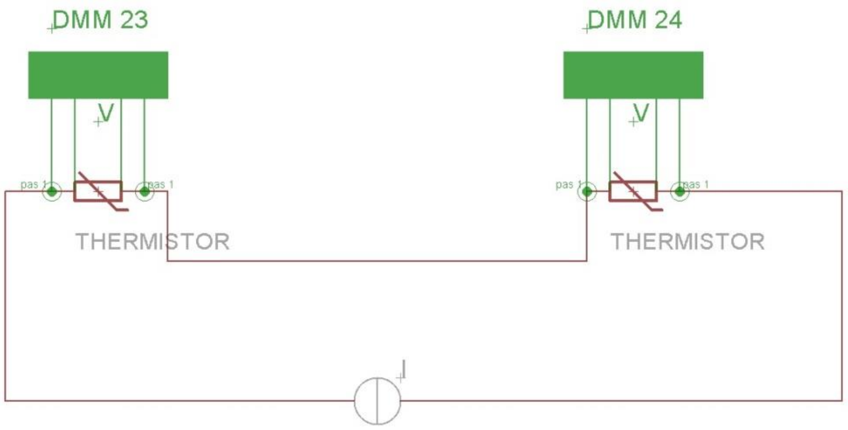

Figure 9: Measurement circuit with external power source and both thermistors connected to their digital multimeters.

The water temperature needs to be stable before measuring the self-heat. This is done by the heat exchange systems as mentioned in § 2.1. The voltage over the thermistor is measured with the digital multi-meter (DMM). Ohm's law represents the resistance as function of the current and the voltage. The resistance of the thermistor is calculated by measuring the voltage over the thermistor. The temperature of the thermistor is determined with the resistance and equation (5). The temperature of the thermistor is measured at different input currents. In this way the self-heat behaviour can be determined.

Because of the temperature change, the resistance of the thermistor will change. The relation between the resistance and the temperature of the thermistor is expressed by equation (5).
The temperature is measured at different current values. When the current increases, the power dissipated in the thermistor will also increase. Therefore the temperature will rise at higher current values.

The temperature is measured at 5, 50, 70, 87, 100 and 122 µA. These points are taken to make sure the dissipated power will increase linear. When increasing the current it takes time for the temperature to stabilize. The stable temperature is measured for 300 seconds. The next step is to increase the current and wait till the temperature is stable again. This process is repeated for the other current values. An example of the measurement is shown in figure 10. The dissipated power in the thermistor is shown above the measured data.

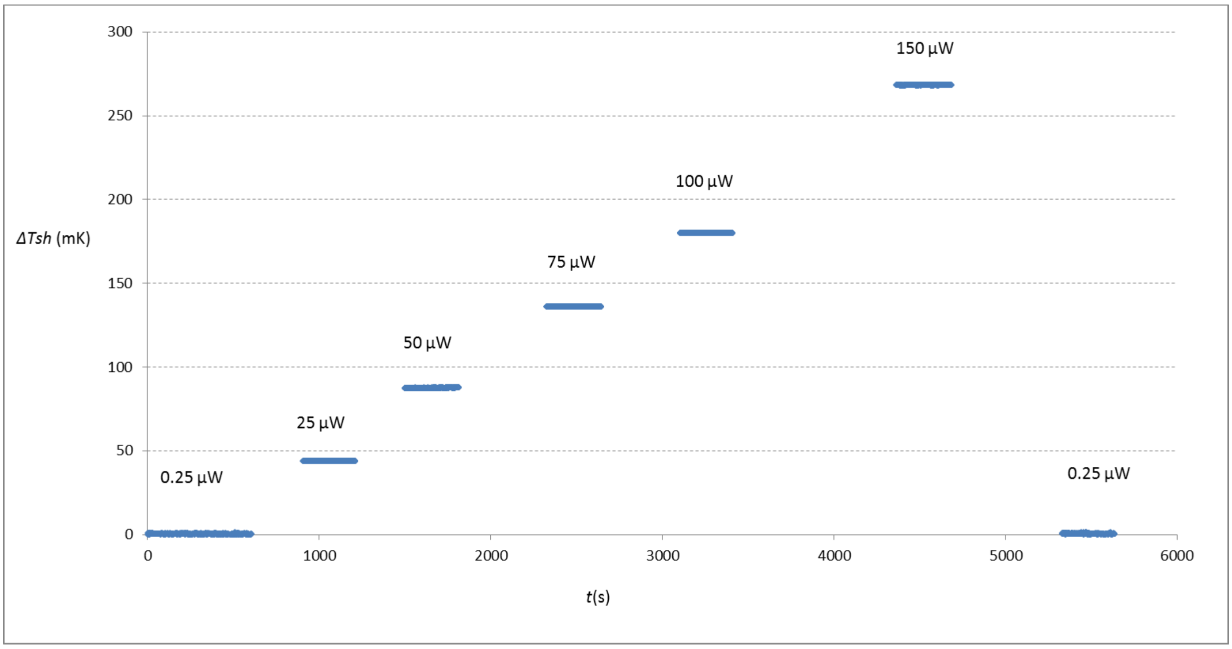

Figure 10: Example of the self-heat measurement, with on de x-axis the time and on the y-axis the temperature change compared to the first temperature.

In this measurement the input current is controlled by an external current source and not by the DMMs. The method only measures the self-heat with a constant input current. For this reason only the self-heat without the OCOMP setting can be measured using this method. This measurement technique is used as a first impression on the behavior of the self-heat of the thermistors. A result of this measurement technique is shown in appendix I.

3.2 Self-heat measurement with parallel resistance

Additional resistors are used with the second measurement method. A parallel resistor is put over the thermistor. Instead of changing the input current, the resistance of the parallel resistor will be changed. In contrast to the first method, there will be no external power source. The DMM's provide an input current of 100 µA. The current through the thermistor will change when the parallel resistor is changed.

The parallel resistors are chosen such that the dissipated power in the thermistor will increase linearly. The greater the value of the parallel resistance, more amperes will go through the thermistor.

The used parallel resistor values are shown in table 1. The associated current that will go through the thermistor is calculated with the following equation:

$$I = I_{DMM} \cdot \frac{R_{par}}{R_{par}+R} \tag{13}$$

With

I	the current through the thermistor	[A]
R_{par}	the resistance of the parallel resistor	[Ω]
R	the resistance of the thermistor	[Ω]

The dissipated power in the thermistor P due to the current is equal to:

$$P = I \cdot R^2 \tag{14}$$

Table 1: The used parallel resistance, the associated current, the dissipated power of the thermistor and the uncertainty of the dissipated power.

Measurement	R_{par} (kΩ)	R (kΩ)	I (µA)	P (µW)	U_P (µW)
1	0.50	9.79	4.9	0.23	2.3E-06
2	5.0	9.78	34	11	1.1E-04
3	10	9.78	51	25	2.5E-04
4	24	9.76	71	50	5.0E-04
5	100	9.74	91	81	8.1E-04
6	-	9.72	100	97	9.7E-04
7	0.50	9.79	4.9	0.23	2.3E-06

The parallel resistors are calibrated first. This is done with the DMMs to which the resistors are connected during the measurement. The calibration is done by measuring the resistance of the parallel resistor for two minutes. The statistics and results are taken into account in the uncertainty budget which are shown in § 4.2.

The resistance of the parallel resistors is calibrated before and after each self-heat measurement. This is done in order to measure any changes in resistance over time. The mean value of the two minute measurement with the associated uncertainty is used.

The resistance of the thermistor is calculated with the following equation:

$$R = \frac{R_{par} \cdot R_m}{R_{par} + R_m} \tag{15}$$

R_m is the total resistance of the parallel resistor and the thermistor. R_m is measured with a DMM. R_{par} is calibrated as mentioned above. The dissipated power in the thermistor will change due to a different parallel resistance. The self-heat temperature is measured for each dissipated power shown in table 1.

This method uses the DMM as the current source. Therefore the OCOMP setting can be used. The self-heat can be determined with the OCOMP on and the OCOMP off. This way the behavior of the self-heat can be determined.

3.3 Self-heat constantfits

The self-heat parameters need to be determined to calculate the ratio between OCOMP on and OCOMP off. The self-heat constant is determined by fitting the temperature change due to the dissipated power in the thermistor. This is done by two different fitting equations. The first fit uses the equations shown in § 2.3. This fit can be explained by use of physics. A second fit is used to compare the results and to make sure the behavior of the fit is correct. The second fit is based on an earlier study on the self-heat of thermistors [3].

The temperature change of the thermistor due to self-heat is measured by measuring the temperature of the thermistor at different current values. The measurement takes place over a couple of hours. During this time, the environment will cause a background drift in the water temperature. The temperature of the environment causes the background. The background drift is described by an offset σ and the temperature change per time unit due to the background drift δ in mK/min. The background drift is approximately 10^{-4} mK/sec.

3.3.1 Fit P versus ΔT_{sh}

The first fit is based on the equations in § 2.3. The fit can be physically explained by the convection and the self-heat. The background drift and the temperature change due to the environment temperature could be seen as a power drift, but a clear physical explanation cannot be given.

When combining the background drift and equation (12), the dissipated power P in the thermistor can be written as:

$$P = (\sigma_1 + \delta_1 \cdot \tau) + \frac{1}{c_{sh}} \cdot \Delta T_{sh} + v \cdot \Delta T_{sh}{}^2 \tag{16}$$

With:

ΔT_{sh}	the temperature change due to the power of the thermistor	[K]
σ_1	the offset of the fit of the drift	[W]
δ_1	the temperature change due to background drift	[W·s^{-1}]
τ	the time after the first measurement	[s]
v	the convection constant	[W·K^{-2}]

Equation (16) is used as a least square fit of the measured time, the dissipated power of the thermistor and temperature change of the thermistor. σ_1 ,δ_1, c_{sh} and v are determined by use of the least square fit.

According to equation (16) the self-heat constant is equal to:

$$c_{sh1} = \left(\frac{P}{\Delta T_{sh}} - \frac{\sigma_1 + \delta_1 \cdot \tau}{\Delta T_{sh}} - v \cdot \Delta T_{sh}\right)^{-1} \tag{17}$$

c_{sh1} is the self-heat constant determined with the fit shown in equation (16). Equation (17) is used to calculate the self-heat constant and is used to determine the uncertainty in the self-heat constant.

3.3.2 Fit ΔT_{sh} versus P

The second fit is shown in equation (18) and describes the change of the temperature of the thermistor as a function of the dissipated power in the thermistor.

$$\Delta T_{sh} = (\sigma_2 + \delta_2 \cdot \tau) + c_{sh} \cdot P + B \cdot P^2 \tag{18}$$

With:

ΔT_{sh}	the temperature change due to the power of the thermistor	[K]
σ_2	the offset of the fit of the drift	[K]
δ_2	the temperature change due to background drift	[$K \cdot s^{-1}$]
τ	the time after the first measurement	[s]
c_{sh}	the self-heat constant	[$K \cdot W^{-1}$]
P	the dissipated power of the thermistor	[W]
B	constant of the linearity of the fit	[$K \cdot W^{-2}$]

Just like the first fit, the second fit desribes the background drift. In §2.3 the temperature change due to the self-heat constant and the dissipated power is given by equation (7). Equation (7) is an approximation. The relation between the self-heat temperature and the dissipated power is not linear. A previous study shows a deviation of the linear relation between the self-heat and the dissipated power in the thermistor. The study shows that the linearity decreases at larger power values.

The study introduces the B-constant. The non-linearity of the self-heat is given by the B-constant in K/W^2. B can be explained as the change of the self-heat constant per watt. According to equation (18), the self-heat constant is equal to:

$$c_{sh2} = \frac{\Delta T_{sh}}{P} - \frac{\sigma_2}{P} - \frac{\delta_2 \cdot \tau}{P} - B \cdot P \tag{19}$$

c_{sh2} is the self-heat constant determined with the equation (19). Equation (19) is used as a fit to determine σ_2, δ_2, C_{sh2} and B.

3.4 Uncertainty budget self-heat constant

The self-heat constant depends on the variables given by equation (17) and (19). The total uncertainty in the self-heat constant therefore depends on the uncertainties in these variables. The uncertainty budget of the self-heat constant is shown in § 4.2.

The contribution of each uncertainty on the total output uncertainty is given by the sensitivity coefficient and the uncertainty of the associated variable. The sensitivity coefficient is determined by the partial derivatives of the variable. The uncertainty of the self-heat constant $U_{C_{sh}}$ is given by the following equation [4] [5].

$$U_{C_{sh}} = \sqrt{\sum |c_i \cdot U_i|^2} \qquad (20)$$

Where c_i is the sensitivity coefficient of a variable. And U_i is the uncertainty of the associated variable.The uncertainty of the self-heat constant determined with the first fit $U_{c_{sh1}}$ is given by equation (21).

$$U_{c_{sh1}} = \sqrt{\left(\frac{\partial C_{sh1}}{\partial T} \cdot U_T\right)^2 + \left(\frac{\partial C_{sh1}}{\partial P} \cdot U_P\right)^2 + \left(\frac{\partial C_{sh1}}{\partial v} \cdot U_v\right)^2 + \left(\frac{\partial C_{sh1}}{\partial \delta_1} \cdot U_{\delta 1}\right)^2 + \left(\frac{\partial C_{sh1}}{\partial \sigma_1} \cdot U_{\sigma 1}\right)^2 + \left(\frac{\partial C_{sh1}}{\partial \tau} \cdot U_\tau\right)^2} \qquad (21)$$

The sensitivity coefficients of the variables used for the first fitting method are shown in table 2.

Table 2: The sensitivity coefficients of the associated variables for the first fitting method.

i	variable	c_i
1	ΔT_{sh}	$-c_{sh}{}^2 \cdot \left(-\frac{P}{\Delta T_{sh}{}^2} + \frac{\sigma_1+\delta_1\tau}{\Delta T_{sh}{}^2} - v\right)$
2	P	$-c_{sh}{}^2 \cdot \frac{1}{\Delta T_{sh}}$
3	v	$-c_{sh}{}^2 \cdot \Delta T_{sh}$
4	δ_1	$-c_{sh}{}^2 \cdot -\frac{\tau}{\Delta T_{sh}}$
5	σ_1	$-c_{sh}{}^2 \cdot -\frac{1}{\Delta T_{sh}}$
6	τ	$-c_{sh}{}^2 \cdot -\frac{\delta 1}{\Delta T_{sh}}$

The uncertainty of the self-heat constant determined with the second fit $U_{C_{sh2}}$ is equal to:

$$U_{Csh2} = \sqrt{\left(\frac{\partial C_{sh2}}{\partial T} \cdot U_T\right)^2 + \left(\frac{\partial C_{sh2}}{\partial P} \cdot U_P\right)^2 + \left(\frac{\partial C_{sh2}}{\partial B} \cdot U_B\right)^2 + \left(\frac{\partial C_{sh2}}{\partial \delta_2} \cdot U_{\delta 2}\right)^2 + \left(\frac{\partial C_{sh2}}{\partial \sigma_2} \cdot U_{\sigma 2}\right)^2 + \left(\frac{\partial C_{sh2}}{\partial \tau} \cdot U_\tau\right)^2} \qquad (22)$$

Table 3 shows the sensitivity coefficients of the variables used in the second fitting equation.

Table 3: The sensitivity coefficients of the variables used in fitting equation 19 .

i	**variable**	c_i
1	ΔT_{sh}	$\frac{1}{P}$
2	P	$-\frac{\Delta T_{sh}}{P^2}+\frac{\sigma_2+\delta_2\tau}{P^2}-B$
3	B	P
4	δ_2	$\frac{\tau}{P}$
5	σ_2	$\frac{1}{P}$
6	τ	$\frac{\delta_2}{P}$

Equation (21) and (22) describe the total absolute uncertainty in the self-heat constant. These equations and the sensitivity coefficients described in table 2 and 3 are used to calculate the uncertainty in the self-heat constant and therefore in the OCOMP on and OCOMP off ratio. The results are shown in the uncertainty budgets in § 4.2. An uncertainty budget is made for both fits.

4 Results

This chapter discusses the results of the self-heat measurements. The results of the two different fits are shown in this chapter.

4.1 Self-heat measurement with a parallel resistance

The measured data is fitted in two different ways as described in § 3.3. The two fits are shown in equation (16) and equation (18).

The used parallel resistance values are show in table 1. The resistance of the thermistor R is calculated on basis of R_m and the value of the parallel resistance R_{par}. The temperature of the thermistor is determined with equation (5). The temperature of the thermistor is measured at different current values. An example of the measurement is shown in figure 11.

Measurements were performed with four different thermistors in two different HPC cells. Cell 1 is shown in figure 4. Cell 1 is the standard cell that is used in the water calorimeter. Cell 2 is a smaller cell. The influence of the size of the cell on the self-heat constant is determined, by doing measurements with two different cells. The four different thermistors are labelled with the following thermistor ID's: VSL13T025, VSL13T033, VSL13T023 and VSL13T026. All the used thermistors are 10 kΩ negative temperature coefficient thermistors.

Figure 11 shows the measurement of the VSL13T025 thermistor. The OCOMP function of the DMM was ON and the thermistor was positioned in cell 1. The measured temperature difference due to the self-heat is given as function of the time along with the associated results of the second fit.

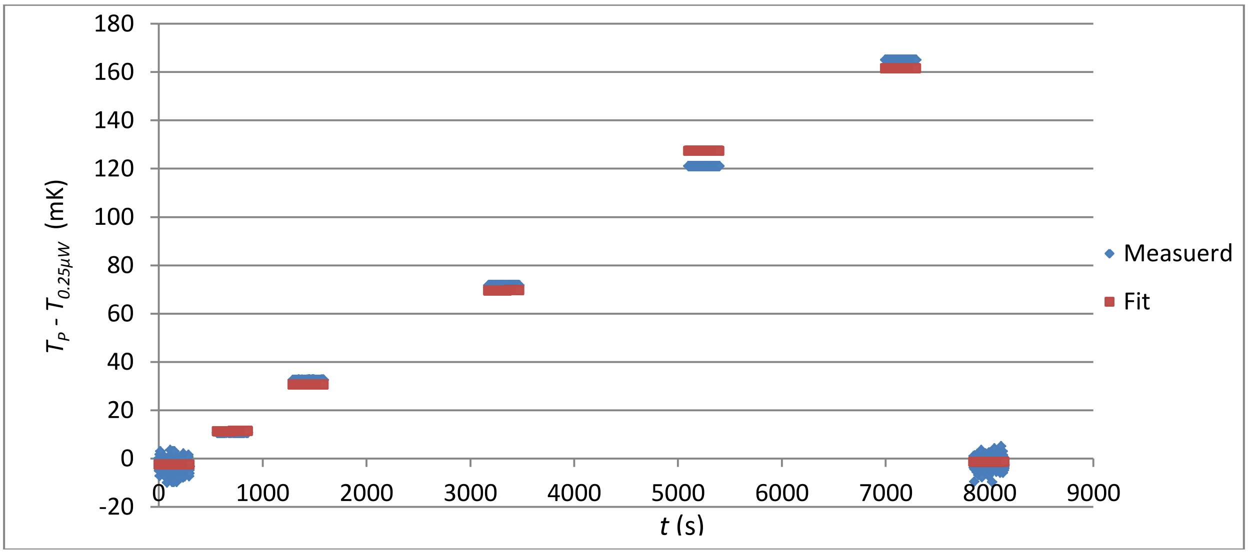

Figure 11: The self-heat temperature plotted against the time. The blue points show the measured temperature change and the red points show the temperature change according to the fit.

The blue dots show the measured temperature change relative to the first measurement point. The first 300 seconds are measured with a parallel resistor of 0.5 kΩ. As shown in table 1 this correspondent with a dissipated power in the thermistor of 0.23 µW. This causes a minimal temperature change due to the self-heat. The temperature change of the thermistor in relation to the 0.5 kΩ point is measured for each parallel resistor for 300 seconds.

The thermistor needs a current to measure the temperature of the water, therefore it is impossible to measure the self-heat temperature at a dissipated power of 0 µW. For this reason the first point is taken as the initial temperature and assumed to be at a self-heat of zero K.

The first fitting method can be explained by using physics. Only the self-heat constant cannot be determined correctly in all cases. The self-heat constant indicates a constant that is independent of the initial temperature of the thermistor. In other words, if the temperature at for example 11.2 µW is taken as the initial temperature instead of the lowest temperature, the self-heat constant would be the same. But the first fitting method consists of a ΔT_{sh} and a $\Delta T_{sh}{}^2$. Therefore the self-heat constant will change if the initial temperature is changed. In the analyse technique of the first fit, the initial temperature is the temperature at the lowest dissipated power, thus the lowest self-heat temperature. In this case the self-heat constant corresponds with the self-heat constant determined with the second fit.

Figure 12 shows the results of the same measurements, only this time the dissipated power is plotted as function of the time. The second fit is used in figure 12.

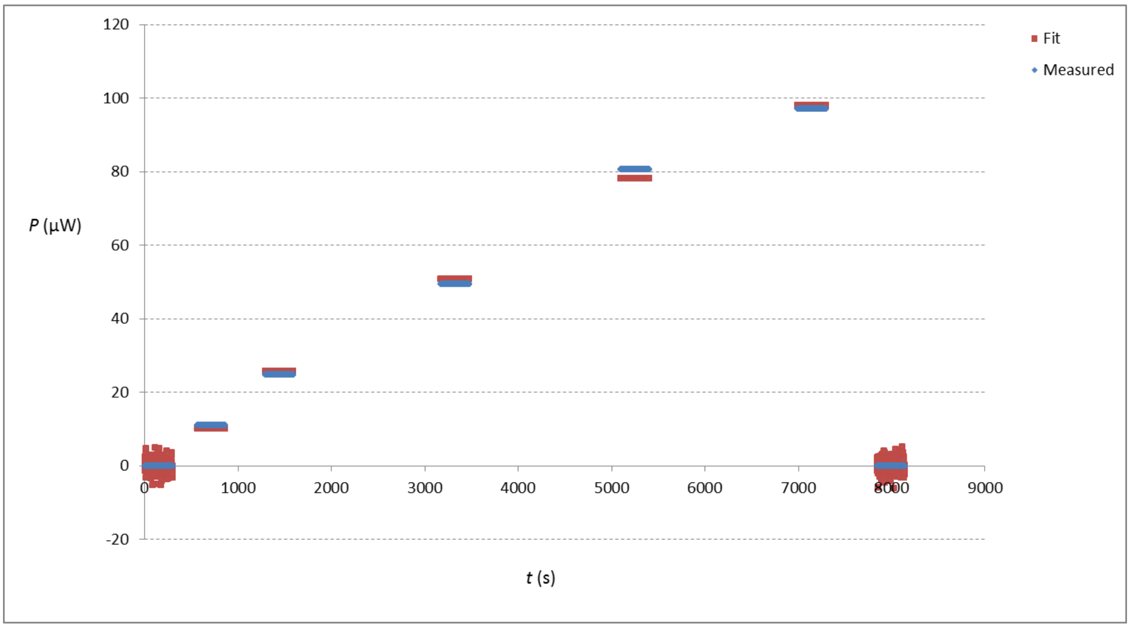

Figure 12: The dissipated power of the thermistor plotted against the time. The blue points show the measured dissipated power and the red points show the temperature change according to the fit.

As shown in figure 11 and 12, the fit correspondents with the measured data. Therefore the constants of the fitting equation can be determined.

Figure 13 shows the residuals of the measured data compared to the fitted data. The results of the fit are subtracted from the results of the measurement. If the fit works correctly the sum of the residuals must be zero. This is the case according to the results.

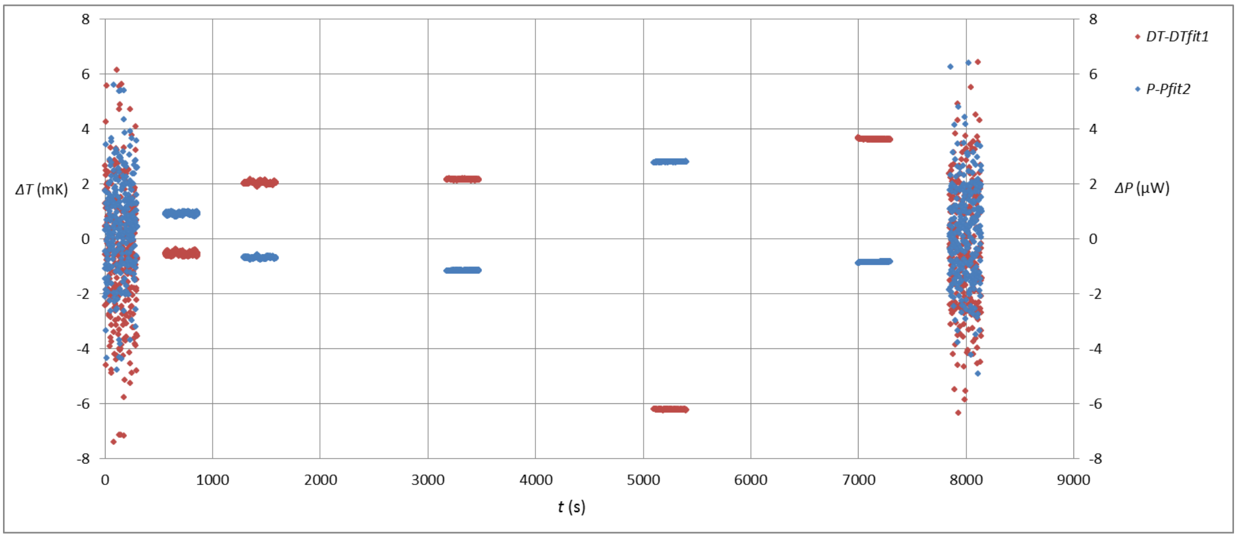

Figure 13: The residential of both fits for the measurement with thermistor VSL 13T025 in cell 2 with OCOMP on.

Figure 11, 12 and figure 13 show a statistical dispersion at the first and last 300 points of the measured data. This is caused by the parallel resistance. The two resistors of 0.5 kΩ have a large standard deviation of approximately 5 ppm. Where the rest of the used parallel resistors have a standard deviation of approximately less than 1 ppm. The influence of the standard deviation of the 0.5 kΩ on the final uncertainty of the self-heat constant is negligible.

4.2 The uncertainty in the self-heat constant

The uncertainty of the self-heat parameter c_{sh} is determined with an uncertainty budget. The uncertainty budget consists of all the variables that are used for determining the c_{sh}. The uncertainty budget for c_{sh1} is shown in table 4. The uncertainty budget shows the value, standard uncertainty, probability distribution, sensitivity coefficient, uncertainty type and the uncertainty component of each variable. The equations and the sensitivity coefficients that are used to determine the uncertainty in the self-heat constant are described in § 3.4.

Table 4: The uncertainty budget of the P versus ΔT_{sh}fit method.

Uncertainty budget C_{sh1}	Variable	Value of quantity	Standard uncertainty	Probability distribution	Sensitivity coefficient	Uncertainty type	Coverage factor	Confidence level	Uncertainty component
Measured Resistance (kΩ)			u_i (ppm)		c_i	-	k	%	$\|c_i u_i\|$(ppm)
1	DMM resolution	x	2.9E-06	rectangular	1	Type B	1	68	2.9E-06
2	DMM calibration	x	6.0E+00	Normal	1	Type B	1	68	6.0
Parallel resistance (kΩ)			u_i (ppm)		c_i	-		%	$\|c_i u_i\|$(ppm)
3	Uncertainty of mean	x	4.3	Normal	1	Type A	1	68	4.3
4	DMM resolution	x	2.9E-06	rectangular	1	Type B	1	68	2.9E-06
5	DMM calibration	x	6.0	Normal	1	Type B	1	68	6.0
Source current DMM	100		u_i (ppm)		c_i	-		%	$\|c_i u_i\|$(ppm)
6	DMM resolution	x	1.0	rectangular	1	Type B	1	68	1.0
7	DMM calibration	x	3.0	Normal	1	Type B	1	68	3.0
Power off thermistor (µW)					c_i	-			u_i (ppm)
8	Uncertainty P (µW)	97.2					1		10
Uncertainty T_{sh}			u_i (ppm)		c_i			%	$\|c_i u_i\|$(ppm)
9	Thermistor Resistance (kΩ)	9331	3.0	Normal	1	Type A	1	68	3.0
10	Uncertainty of β	3090	3.0	Normal	1	Type A	1	68	3.0
11	Uncertainty of R_0	9382	2.0	Normal	1	Type A	1	68	2.0
Total uncertainty in T_{sh}									$\|c_i u_i\|$(ppm)
12	Uncertainty T_{sh} (mK)	182					1		11
Other uncertainties			u_i (%)		c_i	-	k	%	$\|c_i u_i\|$(ppm)
13	Offset (mK)	2.4E-02	221	Normal	1.2E-02	Type A	1	68	1.2E+03
14	drift (mK/min)	-1.9E-05	56.3	Normal	1.6E+00	Type A	1	68	3.1E+01
15	v constant	-5.7E-04	0.9	Normal	4.1E+02	Type A	1	68	8.0E+03
16	Time (min)	1.3E+02	1.0E-03	Normal	2.4E-07	Type A	1	68	0.0E+00
17	ΔT_{sh} (mK)	1.8E+02	1.1E-03	Normal	-5.3E-03	Type A	1	68	-1.9E+01
18	P_{th} (µW)	9.7E+01	1.0E-05	Normal	1.2E-02	Type A	1	68	8.0E-08
Total uncertainty in self-heat constant							k	%	$\|c_i u_i\|$(%)
19	C_{sh1} (mK/µW)	1.5					1	68	8.1

All the used variables are shown in the uncertainty budget. The uncertainty budget also shows the type of uncertainty. Type A uncertainty's are determined by statistical means. The type A method is applicable for evaluating the uncertainty by statistical analysis of a series of measurements. Type A will be used for experimental data and measurements. Type B evaluation is a method other than statistical analyses of a series of measurements. The type B evaluation is based on calibrations of the used materials and equipment.

The most important uncertainties are shown in yellow. The relative uncertainty in the c_{sh1} is shown in the last row and column of table 4. The relative uncertainty in c_{sh1} is 8.1 % with k = 1. The coverage factor k = 1 corresponds with a confidence level of 68 %.

The uncertainty budget of c_{sh2} is shown in table 5. The uncertainty budget consist the same information of each variable as the uncertainty budget for c_{sh1}.

Table 5: The uncertainty budget of the ΔT_{sh} versus P fit method.

Uncertainty budget C_{sh2}	Variable	Value of quantity	Standard uncertainty	Probability distribution	Sensitivity coefficient	Uncertainty type	Coverage factor	Confidence level	Uncertainty component
Measured Resistance (kΩ)			u_i (ppm)		c_i	-		%	$\|c_i u_i\|$ (ppm)
1	DMM resolution	x	2.9E-06	rectangular	1	Type B	1	68	2.9E-06
2	DMM calibration	x	6.0E+00	Normal	1	Type B	1	68	6.0
Parallel resistance (kΩ)			u_i (ppm)		c_i	-		%	$\|c_i u_i\|$ (ppm)
3	Uncertainty of mean	x	4.3	Normal	1	Type A	1	68	4.3
4	DMM resolution	x	2.9E-06	rectangular	1	Type B	1	68	2.9E-06
5	DMM calibration	x	6.0	Normal	1	Type B	1	68	6.0
Source current DMM	100		u_i (ppm)		c_i	-		%	$\|c_i u_i\|$ (ppm)
6	DMM resolution	x	1.0	rectangular	1	Type B	1	68	1.0
7	DMM calibration	x	3.0	Normal	1	Type B	1	68	3.0
Power off thermistor (µW)					c_i	-			u_i (ppm)
8	Uncertainty P (µW)	97.2					1		10
Uncertainty T_{sh}			u_i (ppm)		c_i			%	$\|c_i u_i\|$ (ppm)
9	Thermistor Resistance (kΩ)	9331	3.0	Normal	*1*	Type A	1	68	3.0
10	Uncertainty of β	3090	3.0	Normal	1	Type A	1	68	3.0
11	Uncertainty of R_0	9382	2.0	Normal	1	Type A	1	68	2.0
Total uncertainty in T_{sh}							k		$\|c_i u_i\|$ (ppm)
12	Uncertainty T_{sh} (mK)	181					1		11
Other uncertainties			u_i (%)		c_i	-		%	$\|c_i u_i\|$ (ppm)
13	Offset (mK)	3.1E+00	1.5E-01	Normal	-1.0E-02	Type A	1	68	1.1E+03
14	drift (mK/min)	-8.0E-06	2.9E+02	Normal	-1.3E+00	Type A	1	68	2.2E+01
15	B constant	6.6E-03	1.4E+00	Normal	-9.7E+01	Type A	1	68	6.4E+03
16	Time (min)	1.3E+02	1.0E-03	Normal	-8.2E-08	Type A	1	68	4.5E-03
17	ΔT_{sh} (mK)	1.8E+02	1.1E-02	Normal	1.0E-02	Type A	1	68	1.1E+00
18	P_{th} (µW)	9.7E+01	1.0E-05	Normal	-2.5E-02	Type A	1	68	1.7E-07
Total uncertainty in self-heat constant							k	%	$\|c_i u_i\|$ (%)
19	Uncertainty C_{sh2} (mK/µW)	1.4					1	68	6.5

The relative uncertainty in the c_{sh2} is shown in the last row and column of table 5. The relative uncertainty in c_{sh2} is 6.5 % with *k* = 1. The coverage factor *k* = 1 corresponds with a confidence level of 68 %.

4.3 The self-heat results

C_{sh1} and the v-constant are determined using equation (16). C_{sh2} and the B-constant are determined with equation (18). Table 6 shows the results of the self-heat constant, the v-constant and the B-constant. It also shows the absolute uncertainty in the self-heat constant, calculated by use of the uncertainty budgets shown in table 4 and table 5.

Table 6: The results of all the self-heat measurements. The table shows the self-heat constant, the associated uncertainty in the self-heat constant and the v- and B -constant.

			Fit 1			Fit 2		
Therm. ID	OCOMP	Cell	C_{sh1}(mK/µK)	U_{Csh1}(mK/µK)	v (nW/mK^2)	C_{sh2}(mK/µK)	U_{Csh2} (mK/µW)	B (µK/µW^2)
VSL13T025	OFF	1	1.45	0.12	-0.77	1.4	0.090	4.4
VSL13T025	OFF	2	1.47	0.12	-0.77	1.4	0.090	4.6
VSL13T025	ON	1	1.30	0.11	-1.05	1.2	0.078	4.8
VSL13T025	ON	2	1.32	0.11	-1.04	1.2	0.078	4.9
Therm. ID	OCOMP	Cell	C_{sh1}(mK/µK)	U_{Csh1}(mK/µK)	v (nW/mK^2)	C_{sh2}(mK/µK)	U_{Csh2} (mK/µW)	B (µK/µW^2)
VSL13T033	OFF	1	2.15	0.17	-0.35	2.1	0.134	6.0
VSL13T033	OFF	2	2.12	0.17	-0.37	2.0	0.131	6.6
VSL13T033	ON	1	1.81	0.15	-0.57	1.7	0.109	6.9
VSL13T033	ON	2	1.80	0.15	-0.57	1.7	0.109	6.7
Therm. ID	OCOMP	Cell	C_{sh1}(mK/µK)	U_{Csh1}(mK/µK)	v (nW/mK^2)	C_{sh2}(mK/µK)	U_{Csh2} (mK/µW)	B (µK/µW^2)
VSL13T023	OFF	1	1.41	0.11	-0.78	1.35	0.088	3.8
VSL13T023	OFF	2	1.43	0.12	-0.72	1.38	0.090	3.5
VSL13T023	ON	1	1.23	0.10	-1.13	1.15	0.075	4.3
VSL13T023	ON	2	1.15	0.09	-1.35	1.05	0.068	4.1
Therm. ID	OCOMP	Cell	C_{sh1}(mK/µK)	U_{Csh1}(mK/µK)	v (nW/mK^2)	C_{sh2}(mK/µK)	U_{Csh2} (mK/µW)	B (µK/µW^2)
VSL13T026	OFF	1	1.52	0.12	-0.63	1.46	0.095	3.9
VSL13T026	OFF	2	1.55	0.13	-0.58	1.49	0.097	3.6
VSL13T026	ON	1	1.39	0.11	-0.80	1.32	0.086	3.9
VSL13T026	ON	2	1.33	0.11	-0.86	1.26	0.082	3.5

The results show that the type of cell does not have influence on the v-constant and the B-constant. The results show that the v-constant is proportional to the self-heat constant. This corresponds with the expectation about the convective heat transfer. The self-heat is the driven force behind convection. The v-constant depends on the self-heat constant and therefore on the OCOMP on or OCOMP off setting.

The B-constant only depends on the thermistor itself. Thus the B-constant can be seen as a thermistor property.

The ratio between OCOMP on and OCOMP off is calculated for each measurement. The ratio between OCOMP on and OCOMP off is equal to the ratio between the self-heat constant at OCOMP on and the self-heat constant at OCOMP off. The results of the ratio between OCOMP on and OCOMP off are shown in table 5.

Table 7: The ratio between OCOMP ON and OCOMP off and the uncertainty in the ratio between OCOMP on and OCOMP off $U_{\mathrm{OCOMP\ ratio}}$.

Therm. ID	Used fit	Cell	*OCOMP ratio*	$U_{\mathit{OCOMP\ ratio}}$
VSL13T025	1	1	0.90	0.073
VSL13T025	1	2	0.90	0.073
VSL13T025	2	1	0.88	0.057
VSL13T025	2	2	0.87	0.057
VSL13T033	1	1	0.84	0.068
VSL13T033	1	2	0.85	0.046
VSL13T033	2	1	0.81	0.053
VSL13T033	2	2	0.83	0.054
VSL13T023	1	1	0.87	0.071
VSL13T023	1	2	0.80	0.065
VSL13T023	2	1	0.85	0.055
VSL13T023	2	2	0.76	0.050
VSL13T026	1	1	0.91	0.074
VSL13T026	1	2	0.86	0.069
VSL13T026	2	1	0.91	0.059
VSL13T026	2	2	0.84	0.055

The uncertainty of the OCOMP ratio is determined with the uncertainty in the self-heat constant. The OCOMP ratio is calculated with use of the self-heat constant as shown in equation (23).

$$OCOMP_{ratio} = \frac{c_{sh_{on}}}{c_{sh_{off}}} \tag{23}$$

The self-heat constant is determined in 32 causes. As shown in table 7. 16 OCOMP ratios are determined with use of the results in table 6. Each OCOMP ratio with the associated absolute uncertainty is shown in table 7.

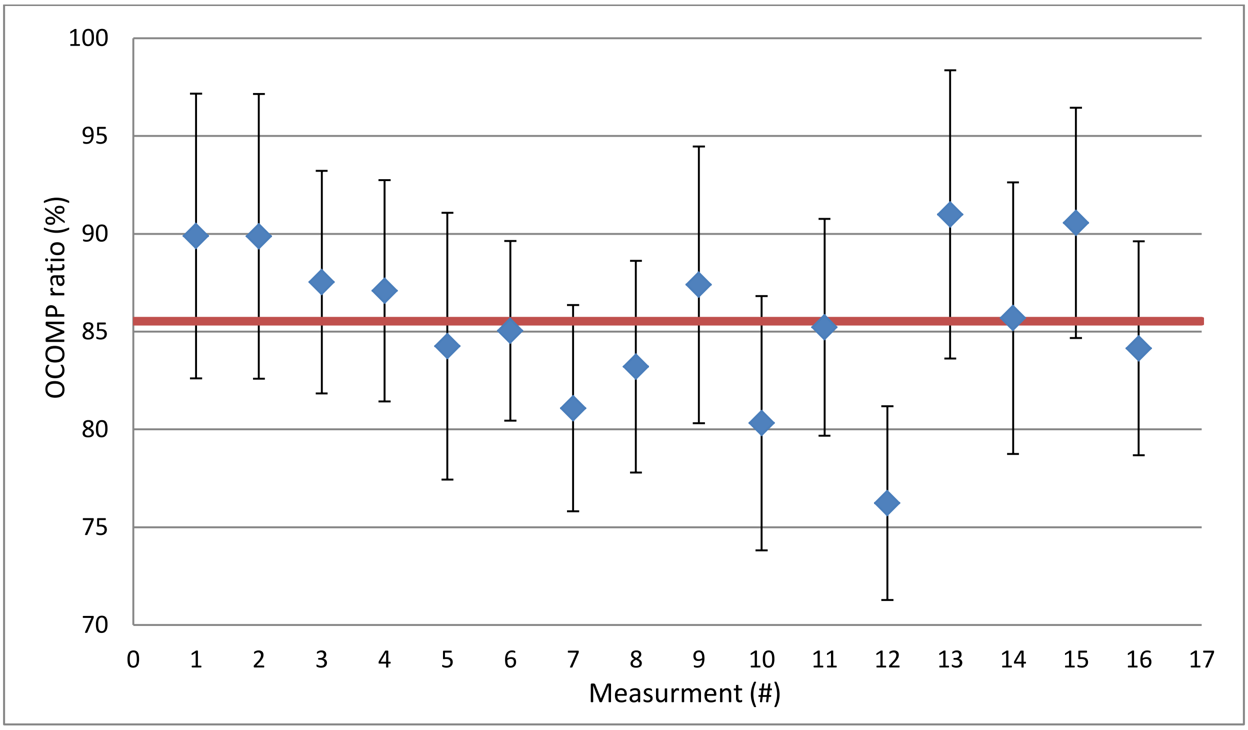

Figure 14: The 16 ratios between OCOMP on and OCOMP off, determined with the self-heat constants. The error bars indicates the uncertainty (*k* = 1) for each result.

The final results of the ratio between OCOMP on and OCOMP off are shown in figure 14. The uncertainty of each measurement point is indicated by the error bars. The red line in figure 14 indicates the mean of the ratio between OCOMP on and OCOMP off.

The average ratio between OCOMP on and OCOMP off is: 85.53 %. The uncertainty budget of the self-heat constant is shown in appendix 6.3.

All the results of the parameters are shown in appendix II. The results of the calibration and the measurement results are obtainable at VSL.

5 Conclusion

This study was conducted to determine the self-heat behaviour of different thermistors under different circumstances in the water calorimeter at VSL. The self-heat of a thermistor is an effect that influences the absorbed-dose-to-water measurements done with the water calorimeter. Therefore it is important to understand the self-heat behaviour of the thermistors in the water calorimeter. The self-heat can be adequately described in two ways: by the self-heat constant and the convection constant *v* or by the dissipated power and a *B*-constant that describes the non-linearity of the self-heat. The research describes two measurement methods that were used to determine the self-heat and their uncertainty budgets.

The effect of the offset compensated ohms (OCOMP setting) of the digital multimeters on the selfheat is determined. The OCOMP setting influences the total temperature change due to self-heat of the thermistors. Therefore it is necessary to describe and determine the OCOMP setting of the digital multimeters. The study describes a measurement technique that can be used to determine the self-heat for both OCOMP on and OCOMP off. The measurement technique is validated by comparing the results with a second measurement technique that can only measure the self-heat without offset compensated ohms using a source meter and voltage meter.

The uncertainties of both fits are described in uncertainty budgets. The sensitivity coefficients of the P versus ΔT_{sh} fit are proportional with c_{sh}^{2}. Therefore the uncertainty in the self-heat depends on the self-heat constant. The uncertainty of the measurement increases for higher self-heat constants. This causes a significantly difference in the uncertainties for each thermistor probe. The sensitivity coefficients in the uncertainty for the ΔT_{sh} versus P fit does not depend on the self-heat constant. The uncertainty will be the same for different thermistors. The relative uncertainty in the DT vs P fit is 6.5 % and the relative uncertainty in the P versus ΔT_{sh} fit is 8.1 %. These properties for both fits led to the recommendation to use the ΔT_{sh} versus P fit for future self-heat measurements.

The results show a statistical dispersion at the first and last 300 measurement points. This is caused by the parallel resistance of 0.5 kΩ. The 0.5 kΩ is used as the zero self-heat point. The second fit does not depend on the zero self-heat point, thus the 0.5 kΩ point is not necessary. The statistical dispersion will be less, by choosing a different parallel resistor as the first point.

The *B*-constant is an important parameter for the self-heat behaviour. The results show a relationship between the *B*-constant and the thermistor probes. More information about the *B*-constant can be obtained by doing measurements with different thermistor probes. The effect of convection can be determined by doing measurements with more high purity cells.

The self-heat behaviour is measured for four different thermistors in two different high purity cells (HPC). The self-heat is determined with the DMM settings OCOMP on and OCOMP off. The data is fitted with two different fitting equations. The uncertainty of the self-heat is determined by two uncertainty budgets, one for each fitting method.

This results in 32 different self-heat measurements and 32 results for each constant with an associated uncertainty. All results are shown in appendix II. The self-heat constants, determined with use of the P_{th} versus ΔT_{sh} fit has an uncertainty of 8.1 % (*k* = 1). The self-heat constants determined with use of the ΔT_{sh} versus P_{th} fit has an uncertainty of 6.5 % (*k* = 1). The self-heat constant of both fits needs to match with each other. The results show that this is the case within the uncertainty.

The variable with the biggest influence on the uncertainty of the self-heat constant in the first fit is the *v*-constant. *v* describes the convection due to the self-heat of the thermistor. The results show that the *v*-constant is proportional with the self-heat constant, this corresponds with the expectations. The results show that the self-heat of the thermistor is the main source for convection. The variable with the biggest influence on the uncertainty of the self-heat constant in the second fit is the *B*-constant. *B* describes the non-linearity of the self-heat behaviour and is introduced in a previous study.

The behaviour of the OCOMP setting is described by the self-heat ratio between OCOMP on and OCOMP off. The ratio is determined by use of the self-heat constant at OCOMP on and OCOMP off. The ratio between OCOMP on and OCOMP off is determined 16 times. This results in an average ratio between OCOMP on and OCOMP off. The average ratio is 0.86 ± 0.08 (*k* = 1).

The results of the self-heat constant and the OCOMP setting of the DMM are used as a correction factor on the absorbed-dose-to-water measurements that are done with the water calorimeter. Because of this research the absorbed-dose-to-water result can be corrected for the self-heat of the thermistors. This leads to a more accurate result in the absorbed-dose-to water measurements. More knowledge about the thermistors leads to a better result in the absorbed-dose-to-water measurements for which the WCM is made.

5.1 Recommendations

The self-heat behaviour was fitted by using two different fitting equations with different parameters. For further measurements and research on the self-heat behaviour, it is necessary to choose one of these fitting methods instead of using both methods. The first fitting method describes the dissipated power in the thermistor as a function of the self-heat. This causes the fit to depend on the initial temperature thus the temperature where the self-heat is assumed to be zero. The second fit does not depend on the initial temperature, therefore the second fit is more applicable.

During the research, work has been done on the processing of the data. A program needs to be written for a better and quicker way to process the data. This can be done by making use of the comprehensive datasheets made in Excel. The quantity and quality of the results will get better by using a more efficient measurement and analyse technique.

List of symbols

β	the thermistor constant	[K]
δ_1	the temperature change due to the background drift	[W·s^{-1}]
δ_2	the temperature change due to background drift	[K·s^{-1}]
v	the convection constant	[W·K^{-2}]
Πk	product of the correction factors	[-]
σ_1	the offset of the drift in the first fit	[W]
σ_2	the offset of the drift in the second fit	[K]
τ	the time after the first measurement	[s]
B	constant of the linearity of the fit	[K·W^{-2}]
c_i	the sensitivity coefficient of a variable	[-]
$c_{p,w}$	the specific heat of water at constant pressure	[4207, 5 J/kg·K]
c_{sh}	the self-heat constant	[K·W^{-1}]
c_{sh1}	the self-heat constant determined with the first fit	[K·W^{-1}]
c_{sh2}	the self-heat constant determined with the second fi	[K·W^{-1}]
d_{body}	the inner diameter of the probes body	[m]
D_{body}	the outer diameter of the probes body	[m]
D_w	the absorbed-dose-to the water	[Gy]
h_{cd}	thermal conduction transfer coefficient	[W·K^{-1}]
h_{cv}	thermal convection transfer coefficient	[W·K^{-1}]
I	the current through the thermistor	[A]
k_{sh}	correction factor for the self-heat	[-]
K	coverage factor	[-]

L_{body}	the length of the probes body	[m]
L_{tip}	the length of the tip of the probe	[m]
$[m \cdot C]_{th}$	the heat capacitance of the thermistor probe	[J·K^{-1}]
P	the dissipated power of the thermistor	[W]
P_{ab}	the absorbed power of the thermistor	[W]
P_{cd}	the power due to conduction	[W]
P_{cv}	the power due to convection	[W]
P_{el}	the electrical power dissipated in the thermistor	[W]
P_r	the power due to radiation	[W]
R	the resistance of the thermistor	[Ω]
R_∞	the thermistor resistance at infinite temperature	[Ω]
R_0	represents the resistance of the thermistor at temperature T_0	[Ω]
R_{par}	the resistance of the parallel resistor	[Ω]
R_m	the measured resistance by the digital multimeters	[Ω]
T	the absolute temperature of the thermistor	[K]
T_0	-	[277.15 K]
T_m	the temperature of the medium	[K]
ΔT_{sh}	the total temperature change of the thermistor due to the self-heat	[K]
$\frac{dT}{dt}$	the temperature change of the thermistor probe per time unit	[K·s^{-1}]
ΔT_w	the temperature change due to radiation	[K]
$U_{C_{sh}}$	the uncertainty in the self-heat constant	[K/W]
U_i	the uncertainty in a variable	[-]

References

[1] de Prez, L.A., (2007). *De NMI standaard voor geabsorbeerde dosis in water in hoogenergetische fotonenstraling*, Delft: VSL

[2] Hamoen, V.C.S., (2013). *Characterization of the self-heat effect of thermistors in the VSL water calorimeter for absorbed dose*, Delft: VSL

[3] Cen, J, (2011). *Self-heat effects of thermistors for absorbed dose measurements*, Delt: VSL

[4] IAEA, (2008).*Measurement uncertainty, a practical guide for secondary standards dosimetry laboratories*, Vienna Austria: IAEA

[5] NMI (2007). *PowerPoint cursus onzekerheidsevaluatie*, Delft: VSL

[6] de Prez, L.A., (2014). *Water calorimeter for tele-therapy applications draft*. Delft: VSL

[7] J. van den Eijnde, M.Schouwenburg (2013). *Praktische stralingshygiëne*, Utrecht

[8] C. Kessler, P.J. Allisy-Roberts, D.T. Burns, P.Roger, L.A. de Prez, J.A. de Pooter, P.M.G. Damen, *Comparison of the standards for absorbed-dose-to water of the VSL and the BIPM for ^{60}Co gamma ray,* Bureau international des Poids et Mesures, Pavillon de Breteuil, Sefres& VSL , Delft, The Netherlands

[9] DMM user manual (2012), *Agilent Technologies 3458A MultimeterUser's Guide*, Loveland, USA: Agilent Technologies Incorporated.

[10] International commission on radiation and measurements (ICRU) (2001), *Dosimetry of high-energy photon beams based on standards of absorbed dose to water.*

[11] de Prez, L.A., Perik, T. (2014), *Megavol nieuwsbrief afdeling RT*, Amsterdam: NKI.

6 Appendix

Extra results are shown in the appendix. For more results, datasheets or calibration the writer of this report need to be contacted.

6.1 Appendix I: Results of the Keithley measurement

Table 5: Results thermistor VSL 13 T 026, Keithley measurement

	B	C_{sh} (mK/µW)	*drift*(mK/min)	*offset*
value:	0.000213574	1.811301083	0.004865151	-0.525732745
uncertainty:	3.33804E-06	0.000449032	0.000275255	0.014038759
uncertainty (%):	1.562945014	0.024790593	5.657681351	-2.670322375

Table 6: Results thermistor VSL 13 T 023, Keithley measurement

Offset on	*B*	C_{sh} (mK/µW)	*drift*(mK/min)	*offset*
value:	0.000161877	1.66975835	0.010055789	-0.413951079
uncertainty:	2.10408E-06	0.000279212	0.000168798	0.008612806
uncertainty (%):	1.299801039	0.01672168	1.678619199	-2.080633896

6.2 Appendix II: The results of the self-heat measurements with parallel resistors,

Cell 1
Thermistor 023
OCOMP OFF
Fit 1

C_{sh1} (mk/μW):	1.41

Variables:	v (μW/mK^2)	1/Csh1 (μW/mK)	drift (μW/min)	Offset (μW)
Values:	-7.7E-04	0.707	-7.3E-05	5.4E-01
Uncertainty	1.1E-05	0.002	1.4E-05	5.8E-02
Uncertainty (%)	1.44	0.24	19.06	10.79

Cell 1
Thermistor 023
OCOMP OFF
Fit 2

Variables:	B (mK/μW^2)	C_{sh2} (μW/mK)	drift (mk/min)	Offset
Values:	3.8E-03	1.35	1.06E-04	-0.53
Uncertainty	7.2E-05	6.48E-03	2.9E-05	0.126071884
Uncertainty (%)	1.91	0.48	26.86	23.88

Cell 1
Thermistor 023
OCOMP ON
Fit 1

C_{sh1}(mk/μW)	1.23

Variables:	v (μW/mK^2)	1/Csh (μW/mK)	drift (μW/min)	Offset (μW)
Values:	-1.1E-03	8.1E-01	-4.4E-05	-1.1E+00
Uncertainty	1.4E-05	2.1E-03	1.7E-05	6.8E-02
Uncertainty (%)	1.28	0.26	37.82	6.19

Cell 1
Thermistor 023
OCOMP ON
Fit 2

Variables:	B (mK/μW^2)	C_{sh2} (μW/mK)	drift (mk/min)	Offset (mK)
Values:	4.27E-03	1.15	4.74E-05	1.76
Uncertainty	7.15E-05	0.01	3.16E-05	0.13
Uncertainty (%)	1.68	0.56	66.63	7.40

Cell 1
Thermistor 026
OCOMP OFF
Fit 1

C_{sh1}(mk/μW)	1.52

Variables:	v (μW/mK^2)	1/Csh (μW/mK)	drift (μW/min)	Offset (μW)
Values:	-6.30E-04	0.66	-1.02E-04	0.45
Uncertainty	8.94E-06	1.58E-03	8.44E-06	0.06
Uncertainty (%)	1.42	0.24	8.29	12.47

Cell 1
Thermistor 026
OCOMP OFF
Fit 2

Variables:	B (mK/μW^2)	C_{sh2} (μW/mK)	drift (mk/min)	Offset (mK)
Values:	3.92E-03	1.46	1.34E-04	-0.29
Uncertainty	6.65E-05	0.01	1.74E-05	0.12
Uncertainty (%)	1.69	0.43	13.06	41.18

Cell 1
Thermistor 026
OCOMP ON
Fit 1

C_{sh1}(mk/µW))	1.39

Variables:	v (µW/mK^2)	1/Csh (µW/mK)	drift (µW/min)	Offset (µW)
Values:	-8.0E-04	7.2E-01	-6.6E-05	-1.2E+00
Uncertainty	1.1E-05	1.9E-03	1.6E-05	6.6E-02
Uncertainty (%)	1.4E+00	2.6E-01	2.4E+01	5.3E+00

Cell 1
Thermistor 026
OCOMP ON
Fit 2

Variables:	B (mK/µW^2)	C_{sh2} (µW/mK)	drift (mk/min)	Offset (mK)
Values:	3.93E-03	1.32E+00	9.01E-05	1.74E+00
Uncertainty	6.96E-05	6.39E-03	3.16E-05	1.30E-01
Uncertainty (%)	1.77E+00	4.84E-01	3.51E+01	7.46E+00

Cell 1
Thermistor 033
OCOMP OFF
Fit 1

C_{sh1}(mk/µW)	2.15

Variables:	v (µW/mK^2)	1/Csh (µW/mK)	drift (µW/min)	Offset (µW)
Values:	-3.45E-04	4.65E-01	-9.80E-05	3.79E-02
Uncertainty	4.32E-06	1.01E-03	7.60E-06	4.99E-02

Uncertainty (%)	1.25E+00	2.18E-01	7.75E+00	1.32E+02

Cell 1
Thermistor 033
OCOMP OFF
Fit 2

Variables:	B (mK/µW^2)	C_{sh2} (µW/mK)	drift (mk/min)	Offset (mK)
Values:	6.01E-03	2.07E+00	2.71E-04	-2.88E-03
Uncertainty	1.10E-04	9.58E-03	2.58E-05	1.75E-01
Uncertainty (%)	1.82E+00	4.64E-01	9.55E+00	6.10E+03

Cell 1
Thermistor 033
OCOMP ON
Fit 1

C_{sh1}(mk/µW)	1.81

Variables:	v (µW/mK^2)	1/Csh (µW/mK)	drift (µW/min)	Offset (µW)
Values:	-5.72E-04	5.51E-01	2.09E-05	6.53E-01
Uncertainty	5.92E-06	1.19E-03	9.60E-06	5.14E-02
Uncertainty (%)	1.03E+00	2.17E-01	4.60E+01	7.87E+00

Cell 1
Thermistor 033
OCOMP ON
Fit 2

Variables:	B (mK/µW^2)	C_{sh2} (µW/mK)	drift (mk/min)	Offset (mK)
Values:	6.87E-03	1.67E+00	-3.99E-05	-6.68E-01
Uncertainty	1.09E-04	9.43E-03	3.05E-05	1.74E-01
Uncertainty (%)	1.58E+00	5.63E-01	7.65E+01	2.60E+01

Cell 1
Thermistor 025
OCOMP OFF
Fit 1

C_{sh1}(mk/µW)	1.45

Variables:	v (µW/mK^2)	1/Csh (µW/mK)	drift (µW/min)	Offset (µW)
Values:	-7.65E-04	6.89E-01	-2.10E-04	-3.64E-01
Uncertainty	1.10E-05	1.90E-03	1.02E-05	6.76E-02
Uncertainty (%)	1.44E+00	2.76E-01	4.86E+00	1.86E+01

Cell 1
Thermistor 025
OCOMP OFF
Fit 2

Variables:	B (mK/µW^2)	C_{sh2} (µW/mK)	drift (mk/min)	Offset (mK)
Values:	4.39E-03	1.38E+00	3.63E-04	6.21E-01
Uncertainty	9.16E-05	8.33E-03	2.34E-05	1.58E-01
Uncertainty (%)	2.08E+00	6.05E-01	6.44E+00	2.54E+01

Cell 1
Thermistor 025
OCOMP ON
Fit 1

C_{sh1}(mk/µW)	1.30

Variables:	v (µW/mK^2)	1/Csh (µW/mK)	drift (µW/min)	Offset (µW)
Values:	-1.05E-03	7.67E-01	-5.77E-05	-1.14E+00
Uncertainty	1.39E-05	2.20E-03	1.30E-05	7.24E-02
Uncertainty (%)	1.33E+00	2.86E-01	2.26E+01	6.36E+00

Cell 1
Thermistor 025
OCOMP ON
Fit 2

Variables:	B (mK/μW^2)	C_{sh2} (μW/mK)	drift (mk/min)	Offset (mK)
Values:	4.84E-03	1.21E+00	8.20E-05	1.61E+00
Uncertainty	9.14E-05	8.25E-03	2.77E-05	1.57E-01
Uncertainty (%)	1.89E+00	6.84E-01	3.38E+01	9.74E+00

Cell 2
Thermistor 023
OCOMP OFF
Fit 1

C_{sh1}(mk/μW)	1.43

Variables:	v (μW/mK^2)	1/Csh (μW/mK)	drift (μW/min)	Offset (μW)
Values:	-7.19E-04	7.01E-01	-2.50E-05	-6.35E-01
Uncertainty	1.14E-05	1.84E-03	1.46E-05	6.31E-02
Uncertainty (%)	1.59E+00	2.62E-01	5.84E+01	9.95E+00

Cell 2
Thermistor 023
OCOMP OFF
Fit 2

Variables:	B (mK/μW^2)	C_{sh2} (μW/mK)	drift (mk/min)	Offset (mK)
Values:	3.51E-03	1.38E+00	4.84E-05	1.09E+00
Uncertainty	7.43E-05	6.72E-03	2.98E-05	1.31E-01
Uncertainty (%)	2.12E+00	4.88E-01	6.15E+01	1.20E+01

Cell 2
Thermistor 023
OCOMP ON
Fit 1

C_{sh1}(mk/μW)	1.15

Variables:	v (μW/mK^2)	1/Csh (μW/mK)	drift (μW/min)	Offset (μW)
Values:	-1.35E-03	8.73E-01	-2.87E-04	2.74E+00
Uncertainty	1.72E-05	2.34E-03	1.92E-05	6.74E-02
Uncertainty (%)	1.28E+00	2.68E-01	6.68E+00	2.46E+00

Cell 2
Thermistor 023
OCOMP ON
Fit 2

Variables:	B (mK/μW^2)	C_{sh2} (μW/mK)	drift (mk/min)	Offset (mK)
Values:	4.10E-03	1.05E+00	3.06E-04	-2.68E+00
Uncertainty	6.74E-05	6.28E-03	3.28E-05	1.26E-01
Uncertainty (%)	1.64E+00	5.98E-01	1.07E+01	4.69E+00

Cell 2
Thermistor 026
OCOMP OFF
Fit 1

C_{sh1}(mk/μW)	1.55

Variables:	v (μW/mK^2)	1/Csh (μW/mK)	drift (μW/min)	Offset (μW)
Values:	-5.75E-04	6.46E-01	-1.18E-04	1.96E-01
Uncertainty	9.02E-06	1.56E-03	1.35E-05	5.75E-02
Uncertainty (%)	1.57E+00	2.42E-01	1.15E+01	2.93E+01

Cell 2
Thermistor 026
OCOMP OFF
Fit 2

Variables:	B (mK/μW^2)	C_{sh2} (μW/mK)	drift (mk/min)	Offset (mK)
Values:	3.54E-03	1.49E+00	1.85E-04	-7.08E-02
Uncertainty	6.97E-05	6.40E-03	2.87E-05	1.26E-01
Uncertainty (%)	1.97E+00	4.28E-01	1.55E+01	1.78E+02

Cell 2
Thermistor 026
OCOMP ON
Fit 1

C_{sh1}(mk/μW)	1.33

Variables:	v (μW/mK^2)	1/Csh (μW/mK)	drift (μW/min)	Offset (μW)
Values:	-8.64E-04	7.54E-01	-2.11E-04	9.15E-01
Uncertainty	1.31E-05	2.04E-03	1.85E-05	6.68E-02
Uncertainty (%)	1.52E+00	2.71E-01	8.76E+00	7.30E+00

Cell 2
Thermistor 026
OCOMP ON
Fit 2

Variables:	B (mK/μW^2)	C_{sh2} (μW/mK)	drift (mk/min)	Offset (mK)
Values:	3.64E-03	1.26E+00	2.73E-04	-1.18E+00
Uncertainty	6.69E-05	6.33E-03	3.35E-05	1.28E-01
Uncertainty (%)	1.84E+00	5.03E-01	1.22E+01	1.08E+01

Cell 2
Thermistor 033
OCOMP OFF
Fit 1

C_{sh1}(mk/µW)	2.12

Variables:	v (µW/mK^2)	1/Csh (µW/mK)	drift (µW/min)	Offset (µW)
Values:	-3.7E-04	4.7E-01	-2.2E-05	-1.2E+00
Uncertainty	3.7E-06	8.8E-04	6.7E-06	4.3E-02
Uncertainty (%)	9.9E-01	1.9E-01	3.1E+01	3.6E+00

Cell 2
Thermistor 033
OCOMP OFF
Fit 2

Variables:	B (mK/µW^2)	C_{sh2} (µW/mK)	drift (mk/min)	Offset
Values:	6.6E-03	2.0E+00	-8.0E-06	3.1E+00
Uncertainty	9.4E-05	8.2E-03	2.3E-05	1.5E-01
Uncertainty (%)	1.4E+00	4.1E-01	2.9E+02	4.8E+00

Cell 2
Thermistor 033
OCOMP ON
Fit 1

C_{sh1} (mk/µW):	1.80

Variables:	v (µW/mK^2)	1/Csh (µW/mK)	drift (µW/min)	Offset (µW)
Values:	-5.70E-04	5.56E-01	-1.91E-05	2.41E-02
Uncertainty	6.05E-06	1.24E-03	1.08E-05	5.34E-02
Uncertainty (%)	1.06E+00	2.22E-01	5.63E+01	2.21E+02

Cell 2
Thermistor 033
OCOMP ON
Fit 2

Variables:	*B* (mK/µW^2)	C_{sh2} (µW/mK)	drift (mk/min)	Offset
Values:	6.65E-03	1.67E+00	2.43E-05	4.62E-01
Uncertainty	1.08E-04	9.41E-03	3.38E-05	1.75E-01
Uncertainty (%)	1.62E+00	5.63E-01	1.39E+02	3.79E+01

Cell 2
Thermistor 025
OCOMP OFF
Fit 1

C_{sh1} (mk/µW):	1.47

Variables:	*v* (µW/mK^2)	1/Csh (µW/mK)	drift (µW/min)	Offset (µW)
Values:	-7.7E-04	6.8E-01	3.3E-05	-1.9E-01
Uncertainty	1.1E-05	1.9E-03	1.1E-05	6.6E-02
Uncertainty (%)	1.4E+00	2.7E-01	3.2E+01	3.4E+01

Cell 2
Thermistor 025
OCOMP OFF
Fit 2

Variables:	*B* (mK/µW^2)	C_{sh2} (µW/mK)	drift (mk/min)	Offset
Values:	4.62E-03	1.38E+00	-8.21E-05	7.83E-01
Uncertainty	8.89E-05	8.11E-03	2.40E-05	1.55E-01
Uncertainty (%)	1.92E+00	5.86E-01	2.92E+01	1.98E+01

Cell 2
Thermistor 025
OCOMP ON
Fit 1

C_{sh1} (mk/µW):	1.32

Variables:	v (µW/mK^2)	1/Csh (µW/mK)	drift (µW/min)	Offset (µW)
Values:	-1.0E-03	7.6E-01	-1.3E-04	2.4E+00
Uncertainty	1.4E-05	2.1E-03	1.4E-05	6.7E-02
Uncertainty (%)	1.3E+00	2.7E-01	1.1E+01	2.8E+00

Cell 2
Thermistor 025
OCOMP ON
Fit 2

Variables:	B (mK/µW^2)	C_{sh2} (µW/mK)	drift (mk/min)	Offset
Values:	4.9E-03	1.2E+00	1.6E-04	-2.9E+00
Uncertainty	9.0E-05	8.2E-03	3.1E-05	1.6E-01
Uncertainty (%)	1.8E+00	6.8E-01	1.9E+01	5.4E+00